

A fractional-spin phase in the power-law Kondo model

Matthias Vojta and Ralf Bulla

Theoretische Physik III, Elektronische Korrelationen und Magnetismus, Universität Augsburg, 86135 Augsburg, Germany
(February 24, 2019)

We consider a Kondo impurity coupled to a fermionic host with a power-law density of states near the Fermi level, $\rho(\epsilon) \sim |\epsilon|^r$, with exponent $r < 0$. Using both perturbative renormalization group (poor man's scaling) and numerical renormalization group methods, we analyze the phase diagram of this model for ferromagnetic and antiferromagnetic Kondo coupling. Both sectors display non-trivial behavior with several stable phases separated by second-order transitions. In particular, on the ferromagnetic side there is a stable intermediate-coupling fixed point with universal properties corresponding to a fractional ground-state spin.

The low-temperature physics of the standard Kondo model, describing a single magnetic impurity embedded in a metal, is by now well understood [1]. For antiferromagnetic coupling between the impurity and the conduction electron spins the effective interaction grows with decreasing temperature. The low-energy behavior is completely determined by a single energy scale, the Kondo temperature T_K , and the impurity spin is fully quenched in the low-temperature limit, $T \ll T_K$. In contrast, for ferromagnetic coupling the effective interaction decreases upon lowering the temperature, leaving the impurity spin essentially decoupled from the environment.

The standard Kondo picture has to be revised if the conduction band density of states (DOS) is not constant near the Fermi level. This is the case in systems with a power-law DOS $\rho(\epsilon) \sim |\epsilon|^r$. Exponents $r > 0$ lead to a vanishing DOS at the Fermi level – such a pseudogap DOS arises in one-dimensional interacting systems, in certain zero-gap semiconductors, and in systems with long-range order where the order parameter has nodes at the Fermi surface, *e.g.*, *p*- and *d*-wave superconductors ($r = 2$ and 1). The pseudogap Kondo problem has attracted a lot of attention during recent years [2–9]. These studies show the existence of a zero-temperature boundary phase transition at a critical antiferromagnetic Kondo coupling, J_c , below which the impurity spin is unscreened even at lowest temperatures. A comprehensive discussion of possible fixed points and their thermodynamic properties has been given by Gonzalez-Buxton and Ingersent [8] based on the numerical renormalization group (NRG) approach.

In this work we investigate a power-law Kondo model for exponents $-1 < r < 0$ which has not been explored before. Negative r implies a diverging low-energy DOS, corresponding to a critical or van-Hove singularity at the Fermi level.

The Kondo Hamiltonian for a spin-1/2 impurity can be written as $H = H_{\text{band}} + H_{\text{int}}$, with

$$H_{\text{int}} = JS \cdot \mathbf{s}_0 + V c_{0\sigma}^\dagger c_{0\sigma} \quad (1)$$

and $H_{\text{band}} = \sum_{\mathbf{k}\alpha} \epsilon_{\mathbf{k}} c_{\mathbf{k}\alpha}^\dagger c_{\mathbf{k}\alpha}$ in standard notation, $\mathbf{s}_0 = \sum_{\mathbf{k}\mathbf{k}'\alpha\beta} c_{\mathbf{k}\alpha}^\dagger \sigma_{\alpha\beta} c_{\mathbf{k}'\beta}$ is the conduction band spin operator

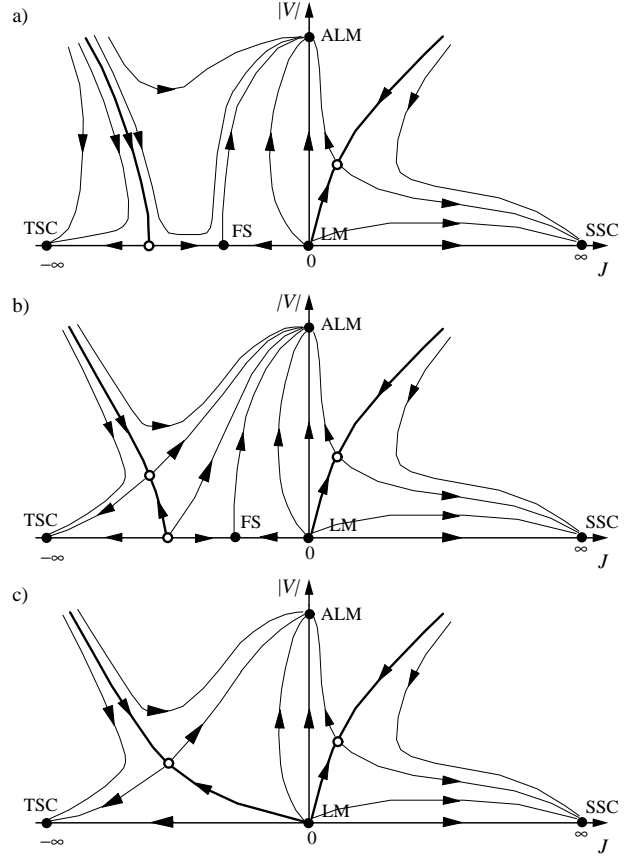


FIG. 1. Schematic renormalization group flows for the power-law Kondo model with $r < 0$, as deduced from NRG calculations (see text). a) $\bar{r}^* < r < 0$, b) $\bar{r}_{\text{max}} < r < \bar{r}^*$, c) $-1 < r < \bar{r}_{\text{max}}$, with NRG estimates of $\bar{r}^* = -0.245 \pm 0.005$, $\bar{r}_{\text{max}} = -0.265 \pm 0.005$. The solid dots denote infrared stable fixed points, the open dots are critical fixed points. FS denotes the infrared stable intermediate-coupling fixed point with fractional spin.

at the impurity site $\mathbf{r}_0 = 0$, and \mathbf{S} denotes the impurity spin operator. For simplicity we will use a conduction band with a symmetric density of states, $\rho(\epsilon) = \rho_0 |\epsilon/D|^r$ for $|\epsilon| < D = 1$, $\rho_0 = (1+r)/(2D)$. Particle-hole (p-h) asymmetry is introduced via the potential scattering term V .

Our findings (Fig. 1) can be summarized as follows: Antiferromagnetic Kondo interactions in the p-h symmetric model ($V = 0$) always flow to a strong-coupling fixed point with a singlet ground state (SSC fixed point) and complete screening of the impurity. The ferromagnetic sector has very rich behavior: large interactions flow to a *ferromagnetic* strong-coupling fixed point with a triplet ground state (TSC). Even more interestingly, for $V = 0$ there exists a *stable* intermediate-coupling fixed point (FS). Its most remarkable property is a Curie response corresponding to a fractional spin,

$$\chi_{\text{imp}} = \frac{\mathcal{C}(r)}{T}, \quad (2)$$

where χ_{imp} is the total impurity contribution to the uniform susceptibility, and \mathcal{C} is a universal, irrational number which depends only on the DOS exponent r . (The $V \neq 0$ behavior is quite complicated as well and will be discussed below.)

Such fractional spin states at intermediate coupling have so far only been found at infrared unstable (critical) fixed points, namely in the pseudogap Kondo model ($r > 0$) [8] and for impurities coupled to quantum-critical magnets [10]. We note that “exotic” states corresponding to stable intermediate-coupling fixed points also occur in multichannel Kondo models [1,11,12]; here, however, the leading term in the impurity susceptibility does not follow a Curie law.

Weak-coupling analysis. We start our considerations with the standard weak-coupling renormalization group treatment (poor man’s scaling [13]), here modified for the power-law Kondo model.

Integrating out a shell of high-energy conduction electrons gives the one-loop renormalization of the Kondo interaction of order J^2 , rescaling of energies and band cut-off Λ leads to an additional renormalization of all couplings proportional to r [2]. Expressed in β functions for the dimensionless running couplings $j = \rho_0 J$ and $v = \rho_0 V$ we have

$$\frac{dj}{d \ln \Lambda} = j(r - j) + \mathcal{O}(j^3), \quad \frac{dv}{d \ln \Lambda} = rv. \quad (3)$$

For $r = 0$ the potential scattering term v remains unchanged whereas positive (negative) Kondo coupling j flows to ∞ (zero) upon decreasing the cut-off. In the pseudogap case, $r > 0$, small j of either sign renormalizes to zero. For small positive r one can deduce a critical fixed point at $J_c = r/\rho_0$, $V_c = 0$, corresponding to the transition between a local moment phase and an antiferromagnetic strong coupling phase in the pseudogap model [2].

Now we turn to $r < 0$: here small j grows for *both* signs of the Kondo coupling. In analogy to the above, on the ferromagnetic side for small negative r , we can predict a fixed point at $J^* = -|r|/\rho_0$ which is now infrared stable (for $V = 0$). The properties of this novel

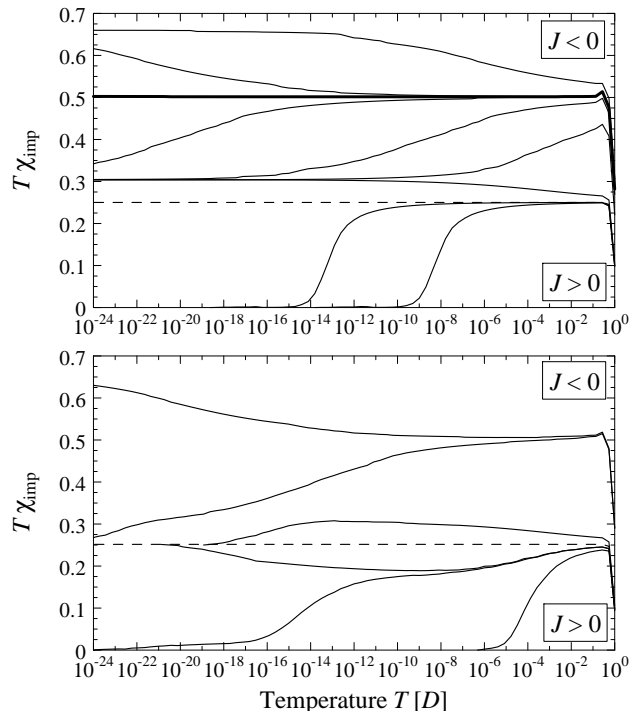


FIG. 2. NRG results [15] for $T\chi_{\text{imp}}$ ($k_B = 1$) of the power-law Kondo model with $r = -0.2$, illustrating the flow in Fig. 1a. The dashed curve shows a free spin $J = 0$ for comparison. a) P-h symmetric case $V = 0$. The thick line corresponds to the critical point at $J_c \simeq -5.6302$. The other curves are for (top to bottom) $J = -7, -5.65, -5.6, -5, -3, -0.1, +0.001, +0.01$. b) Small asymmetry $V \neq 0$. Shown are (top to bottom) $(J, V) = (-7, 0.75), (-7, 0.8), (-0.1, 0.001), (0.045, 0.1), (0.046, 0.1), (0.1, 0.1)$.

intermediate-coupling fixed point are perturbatively accessible in a double expansion in j and r . In principle the calculation of higher-order terms in this expansion is possible; it does, however, not provide information about the fixed point structure for large negative r nor about the flow of large initial couplings J .

Numerical results. To verify the above picture and investigate the strong-coupling behavior, we have performed extensive studies of the power-law Kondo model using the NRG technique [14]. We have found a number of (meta)stable fixed points, with properties listed in the following:

(LM) The symmetric local-moment fixed point corresponds to the system with a decoupled impurity, $J = V = 0$. The impurity susceptibility is $T\chi_{\text{imp}} = 1/4$, the entropy $S_{\text{imp}} = \ln 2$. This fixed point is unstable both w.r.t. to finite J and V , which follows from (3). The instability against potential scattering can be easily understood: finite V leads to a pole in the scattering T matrix which creates a local (anti)bound state, leading to the ALM behavior below.

(ALM) An additional asymmetric local-moment fixed point exists, corresponding to $J = 0$ and $|V| = \infty$; here the conduction electron site next to the impurity is either

doubly occupied or empty. The impurity thermodynamic properties are similar to the LM fixed point.

(SSC) The singlet strong-coupling fixed point is reached for positive J and small $|V|$, it corresponds to $J = \infty$, $V = 0$ and displays a fully quenched spin with $T\chi_{\text{imp}} = 0$, $S_{\text{imp}} = 0$. (The leading term in χ_{imp} has the form T^{-r} , *i.e.*, the impurity susceptibility itself vanishes in the zero-temperature limit.) In contrast to the power-law model with $r > 0$, this fixed point is stable w.r.t. p-h symmetry breaking.

(TSC) A triplet strong-coupling fixed is reached for large negative J , its properties follow from $J = -\infty$, $V = 0$ as $T\chi_{\text{imp}} = 2/3$, $S_{\text{imp}} = \ln 3$. This fixed point is also stable against finite V .

(FS) The new, fractional-spin fixed point exists for small $r < 0$ and is reached for small $J < 0$, $V = 0$. It features a non-trivial r -dependent value of $T\chi_{\text{imp}}$; it is unstable against non-zero potential scattering.

In Fig. 2 we display the temperature dependence of $T\chi_{\text{imp}}$ for different Kondo couplings J and a fixed DOS exponent $r = -0.2$, which puts the model in the interval $\bar{r}^* < r < 0$, with the flow diagram depicted in Fig. 1a. The p-h symmetric case $V = 0$ is shown in Fig. 2a. Positive values of J lead to a fully quenched spin in the low-temperature limit. The ‘‘Kondo’’ temperature characterizing the flow to strong coupling depends in a power-law fashion on J , $T_K \sim D(\rho_0 J)^\alpha$, with the leading term being $\alpha = 1/r$. The behavior is in contrast to the exponential dependence $T_K(J)$ in the metallic $r = 0$ case, reflecting the fact that for $r < 0$ antiferromagnetic J is a relevant rather than a marginally relevant perturbation of the LM fixed point.

Turning to negative values of J , we see that all small ferromagnetic values of the initial coupling yield a flow to the predicted intermediate-coupling fixed point, characterized by a universal Curie behavior of the impurity susceptibility, here $T\chi_{\text{imp}} \approx 0.30$. Interestingly, the basin of attraction of this fixed point does not extend to arbitrarily large $|J|$: large ferromagnetic couplings flow to a different stable fixed point with $T\chi_{\text{imp}} = 2/3$ – this is the triplet TSC fixed point. The boundary quantum phase transition between the fractional spin phase and the triplet phase appears to be second order, and consequently there is an additional unstable p-h symmetric fixed point (thick line in Fig. 2a), separating the FS and TSC regimes.

Switching on potential scattering, Fig. 2b, we find that the LM and FS fixed points are unstable w.r.t. p-h symmetry breaking, and both yield flows towards the ALM fixed point. (Note, however, that $T\chi_{\text{imp}} = 1/4$ for both the LM and the ALM fixed point.) In contrast, both strong-coupling fixed points as well as the critical point between TSC and FS are stable w.r.t. finite V (Fig. 1a). On the antiferromagnetic side, finite V suppresses Kondo screening, leading to another non-trivial transition between the SSC and ALM phases, with an

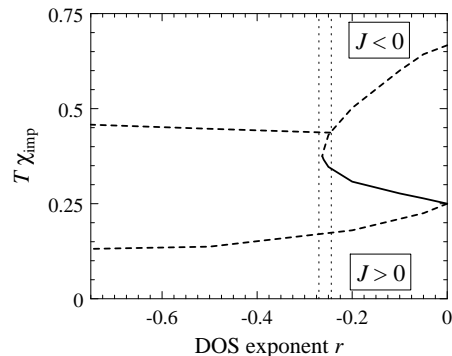


FIG. 3. Values of $T\chi_{\text{imp}}$ at the intermediate-coupling fixed points deduced from NRG [15] as function of the DOS exponent r . Solid: Stable fixed point (FS). Dashed: Critical fixed points. The vertical dotted lines mark the values of $\bar{r}^* \approx -0.245$ and $\bar{r}_{\text{max}} \approx -0.265$.

associated p-h asymmetric critical fixed point at positive J (here $T\chi_{\text{imp}} \approx 0.18$ in Fig. 2b).

Our numerical investigation shows that the described fixed point structure on the ferromagnetic side changes for more negative r values. With decreasing $r < 0$, first the critical fixed point between TSC and FS becomes unstable w.r.t. broken p-h symmetry, and a second critical fixed point with finite asymmetry appears. This means that at a value $r = \bar{r}^*$ the critical fixed point splits, and the transition between TSC and ALM is now governed by the new asymmetric critical point. The resulting renormalization group flow is shown in Fig. 1b. (Strictly speaking, each described fixed point at finite $|V|$ represents a pair of fixed points, which are trivially related by a p-h transformation.)

Upon further decreasing r , the ferromagnetic p-h symmetric critical fixed point moves to smaller couplings, towards the stable FS fixed point. At a certain value $r = \bar{r}_{\text{max}}$ both fixed points meet and disappear (!). This implies that for $r < \bar{r}_{\text{max}}$ and $V = 0$ any negative value of J flows to strong coupling, *i.e.*, leads to a triplet state between the impurity and the conduction electrons. At finite p-h asymmetry, there is still a transition between a local moment and ferromagnetic strong coupling phase, and the critical behavior is governed by a single critical fixed point at finite asymmetry, see Fig. 1c. The above changes do not influence the structure of the flow diagram on the antiferromagnetic side.

The Curie part of the impurity susceptibility, $T\chi_{\text{imp}}$, of the various intermediate-coupling fixed points is shown in Fig. 3. This illustrates nicely the splitting of the unstable ferromagnetic fixed point at $r = \bar{r}^*$ and the collapse of the two fixed points at $r = \bar{r}_{\text{max}}$. A preliminary analysis of the NRG fixed point corresponding to the FS phase shows that it *cannot* be described in terms of non-interacting particles – in contrast to, *e.g.*, the two-channel Kondo fixed point which allows for a Majorana fermion description [12].

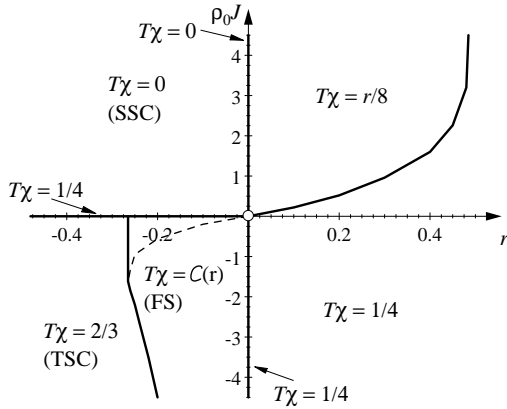


FIG. 4. Phases of the symmetric power-law Kondo model in the $(\rho_0 J) - r$ plane ($V = 0$), with the values of $T\chi_{\text{imp}}$ characterizing each phase. The $r > 0$ sector has been explored, *e.g.*, in Refs. [2,7,8]; the $r < 0$ sector is covered by the present results. Phase transitions (at fixed r) are tuned by moving along vertical lines; all transitions at finite J are of second order; the $J = 0$, $r = 0$ point is the well-known Kosterlitz-Thouless transition of the metallic Kondo model. Solid lines are phase boundaries; the dashed line within the fractional-spin phase (FS) denotes the location of the intermediate-coupling fixed point (estimated from NRG).

The ferromagnetic side of the flow diagrams in Fig. 1 shows some superficial similarity to the antiferromagnetic $r > 0$ situation [8]: Also in this case, two critical fixed points coexist over a certain range of DOS exponents, $r^* < r < r_{\text{max}}$. However, there are crucial differences between the present $r < 0$, $J < 0$ case and the $r > 0$, $J > 0$ regime studied in Ref. [8]: First, the novel stable intermediate-coupling phase FS has no counterpart for $r > 0$. Second, in the $r < 0$ case the weak (strong) coupling fixed points are unstable (stable) w.r.t. to p-h symmetry breaking; for $r > 0$ this is reversed.

Fig. 4 summarizes the phase diagram for the p-h symmetric power-law Kondo model for both signs of the exponent r and both signs of J . The line through the origin describes the fixed points which can be deduced from the weak-coupling equations (3) – note that the line of critical fixed points for $r > 0$ has the same initial slope as the line of stable fixed points for $r < 0$.

In the vicinity of each critical point one can define an energy scale T^* , which vanishes at the transition, and defines the crossover energy above which quantum-critical behavior is observed [16]. We note, however, that on the ferromagnetic side simple one-parameter scaling (as function of T/T^* and ω/T^*) can only be expected for $V = 0$ and $\bar{r}_{\text{max}} < r < 0$ and for $V \neq 0$ and $-1 < r < \bar{r}^*$. In contrast, in the asymmetric case for $\bar{r}^* < r < 0$ the $J < 0$ critical behavior is governed by the symmetric multicritical point (Fig. 1a), leading to two distinct energy scales vanishing at the transition. (This situation is similar to the behavior for small positive r [8].) We have numerically checked the scaling behavior of $T\chi_{\text{imp}}$ and the con-

duction electron T matrix, details will appear elsewhere.

In closing, we mention that the discussed power-law Kondo model is not only of purely theoretical interest: Besides describing “real” magnetic impurities – where a power law DOS can occur due to band structure effects such as van-Hove singularities – effective single-impurity models arise in the context of lattice models in the limit of infinite dimensions (dynamical mean-field theory [17]). Here, the DOS of the effective embedding medium is determined from a self-consistency condition, which can *e.g.* generate a power-law DOS at a critical point of the lattice model. These possibilities, together with the arising non-Fermi-liquid behavior, will be investigated in the future.

We thank M. Glossop, S. Kehrein, and Th. Pruschke for valuable discussions. This research was supported by the DFG through SFB 484.

-
- [1] A. C. Hewson, *The Kondo Problem to Heavy Fermions*, Cambridge University Press, Cambridge (1997).
 - [2] D. Withoff and E. Fradkin, Phys. Rev. Lett. **64**, 1835 (1990)
 - [3] L. S. Borkowski and P. J. Hirschfeld, Phys. Rev. B **46**, 9274 (1992); G.-M. Zhang *et al.*, Phys. Rev. Lett. **86**, 704 (2001).
 - [4] C. R. Cassanello and E. Fradkin, Phys. Rev. B **53**, 15079 (1996) and **56**, 11246 (1997).
 - [5] K. Chen and C. Jayaprakash, J. Phys.: Condens. Matter **7**, L491 (1995).
 - [6] R. Bulla, T. Pruschke, and A. C. Hewson, J. Phys.: Condens. Matter **9**, 10463 (1997), R. Bulla, M. T. Glossop, D. E. Logan, and T. Pruschke, *ibid* **12**, 4899 (2000).
 - [7] K. Ingersent, Phys. Rev. B **54**, 11936 (1996); K. Ingersent and Q. Si, cond-mat/0109417.
 - [8] C. Gonzalez-Buxton and K. Ingersent, Phys. Rev. B **57**, 14254 (1998).
 - [9] M. Vojta, Phys. Rev. Lett. **87**, 097202 (2001).
 - [10] S. Sachdev, C. Buragohain, and M. Vojta, Science **286**, 2479 (1999); M. Vojta, C. Buragohain, and S. Sachdev, Phys. Rev. B **61**, 15152 (2000).
 - [11] P. Nozières and A. Blandin, J. Phys. (Paris) **41**, 193 (1980).
 - [12] R. Bulla, A. C. Hewson, and G.-M. Zhang, Phys. Rev. B **56**, 11721 (1997), and references therein.
 - [13] P. W. Anderson, J. Phys. C **3**, 2436 (1970).
 - [14] K. G. Wilson, Rev. Mod. Phys. **47**, 773 (1975).
 - [15] The values of $T\chi_{\text{imp}}$, S_{imp} are quite sensitive to the truncation of the Hilbert space, *i.e.*, the number of states, N_s , kept in each NRG step. Most data shown are for $N_s = 650$ and a discretization parameter $\Lambda = 2$.
 - [16] S. Sachdev, *Quantum Phase Transitions*, Cambridge University Press, Cambridge (1999).
 - [17] W. Metzner and D. Vollhardt, Phys. Rev. Lett. **62**, 324 (1989); A. Georges, G. Kotliar, W. Krauth and M. J. Rozenberg, Rev. Mod. Phys. **68**, 13 (1996).